High Frequency Modes in Vortex-State Nanomagnets

B. A. Ivanov[1] and C. E. Zaspel[2]

[1]*Institute of Magnetism, NASU, Kiev 03142, Ukraine*

[2]*Department of Environmental Sciences, University of Montana-Western, Dillon, MT 59725, USA*

(Received 22 October 2004; published 21 January 2005)

The magnon mode excitation spectrum is obtained from a linearized set of Landau-Lifshitz equations for vortex ground state cylindrical nanomagnets in an external magnetic field. It is shown that there is a rich spectrum of doublet states, and the splitting can be amplified in an external magnetic field.

DOI: 10.1103/PhysRevLett.94.027205 PACS numbers: 75.75.+a, 75.30.Ds, 75.40.Gb

Magnetic nanoparticles arranged in an array have been proposed for use in high density magnetic information storage; however, ''high density'' implies that the magnetic dipolar interaction between single particles can possibly result in information loss. These problems arising from the interactions between single elements can be minimized through the use of nanoparticles having very small magnetic moments in their ground states. Some of the best candidates are dots and rings made from a soft magnetic material such as permalloy, which has a vortex ground state [1,2] owing to the competition between the exchange and the magnetostatic interactions.

For technical applications, it is necessary to understand the dynamic response of the vortex state in both rings and dots to external pulses, thermal fluctuations, and interactions between elements. A starting point in the study of the dynamics of these systems is a determination of the magnon mode frequencies and mode structures. There have been recent experimental techniques developed to determine mode frequencies, such as Brillouin light scattering (BLS) [3]; recently, time-resolved Kerr microscopy [4,5] has been used to observe the low-frequency gyrotropic mode as well as higher frequency modes and their node structures, and x-ray imaging techniques [6] have been used to directly observe how the core magnetization affects the gyrotropic mode.

In this Letter a general method is presented that is used to obtain the frequencies and mode structure of all modes in both dots and rings. It is shown that the higher frequency modes can be doublets and a static external magnetic field along the particle symmetry axis amplifies the doublet splitting.

The energy W of the vortex-state element in an external field $\vec{H}_0$ is an integral over the element volume of the energy density

$$w(\nabla\vec{M}, \vec{M}) = \frac{A}{2M_s^2}(\nabla\vec{M})^2 - \frac{1}{2}\vec{M}\vec{H}_m - \vec{M}\vec{H}_0, \quad (1)$$

where $\vec{M}$ is the magnetization and M_s is the saturation magnetization. The first term in Eq. (1) is the contribution from the exchange interaction, which is short-range and local in nature, and the second term contains the magnetostatic field, $\vec{H}_m$. The sources of this field are both volume charges arising from $\nabla\cdot\vec{M}$ and surface charges from the component of $\vec{M}$ normal to the surface. The easiest source of magnetostatic charge to consider is the surface M_z at the two faces of the cylinder, where the z direction is defined by the cylinder axis. Then for thin enough structures these surface charges give the energy density $-(1/2)\vec{M}\cdot\vec{H}_m = 2\pi M_z^2$. In the expression for the energy this corresponds to the easy-plane ferromagnet, which is local in nature. The rest of the magnetic charges produce nonlocal fields, which can be obtained from the potential, $\vec{H}_m = -\nabla\Phi$. The potentials from the volume and edge surface magnetostatic charges are known to be

$$\Phi_v = \int \frac{\nabla\cdot\vec{M}(\vec{r}')}{|\vec{r}-\vec{r}'|} r'dr'd\chi'dz',$$
$$\Phi_s = -R\int \frac{\hat{r}\cdot\vec{M}(R)}{|\vec{r}-R\hat{r}|} d\chi'dz', \quad (2)$$

where $(r-\vec{r}')^2 = r^2 + r'^2 - 2rr'\cos(\chi-\chi') + (z-z')^2$, and the integration is over the dot volume, with r and χ defining a cylindrical coordinate system. The equations of motion for the components of the magnetization

$$\frac{\partial\vec{M}}{\partial t} = \gamma\cdot\vec{M}\times\frac{\delta W}{\delta\vec{M}},$$
$$\frac{\delta W}{\delta\vec{M}} = -\frac{A}{M_s^2}\nabla^2\vec{M} + (4\pi M_z - H_0)\hat{\vec{z}} - H_{\text{edge}} - \vec{H}_{\text{vol}}, \quad (3)$$

where $\gamma = g\mu_B/\hbar$, $g \approx 2$ is the gyromagnetic ratio, μ_B is the Bohr magneton, and the nonlocal part of magnetostatic field has been separated into the edge and volume contributions. The static equations give the vortex structure for dot thickness, L, much smaller than the cylinder radius R ($L \ll R$) having the general form $\theta = \theta_0(r)$, $\phi = \chi + \pi/2$, where θ and ϕ are the polar and azimuthal angles of magnetization with respect to the z axis, and (r, χ) are polar coordinates in the dot plane. The function $\theta_0(r)$ is described by the equation $\theta_0'' + \theta_0'/\xi + \sin\theta_0\cos\theta_0(1 - 1/\xi^2) = h\sin\theta_0$, where $\theta_0' = d\theta_0/d\xi$, $\xi = r/l_0$, $l_0 = \sqrt{A/4\pi M_s^2}$ is exchange length and $h = H_0/4\pi M_s$ is a dimensionless external field parameter. This gives the out-of-plane vortex structure with $\cos\theta_0(0) = \pm 1$, and with vortex ''cone-state'' [7] asymptotics far from the vortex core, at $r \gg l_0$,

$$\cos\theta_0(\xi) = h[1 + (l_0/r^2)]$$
$$\text{for } h \neq 0, \cos\theta_0(\xi) \propto \exp(-r/l_0) \quad \text{for } h = 0. \tag{4}$$

To investigate the magnon modes, we will consider small oscillations about the vortex ground state. The magnetization will include small deviations of θ from the vortex ground state, $\theta = \theta_0(r) + \vartheta$, as well as a radial component, μ

$$M_s[\mu\hat{\vec{r}} + (\sin\theta_0 + \vartheta\cos\theta_0)\hat{\vec{\chi}} + (\cos\theta_0 - \vartheta\sin\theta_0)\hat{\vec{z}}], \tag{5}$$

and the equations of motion for the functions $\vartheta(r, \chi, t)$ and $\mu(r, \chi, t)$ are obtained by linearization of (3). Notice that Eq. (3) has edge and volume contributions to the magnetostatic field. In the following it is shown that the edge field will result in a effective boundary conditions and the volume field will only appear in the equations of motion for the small deviations.

We begin with the key ansatz [8]

$$\vartheta(r, \chi, t) = f(r)\cos(m\chi - \omega t)$$
$$\text{and} \quad \mu(r, \chi, t) = g(r)\sin(m\chi - \omega t), \tag{6}$$

separating the radial and azimuthal parts of the deviations. The dynamic equations for the small deviations give the eigenvalue problem

$$\Omega f = \hat{H}_1 g + \hat{V} f + \hat{U}_1 \tag{7a}$$
$$\Omega g = \hat{H}_2 f + \hat{V} g + U_2, \tag{7b}$$

where $\Omega = \omega/4\pi\gamma M_s$ is a dimensionless magnon frequency, and the operators are defined by

$$\hat{H}_1 = -\hat{\Delta}_m + l_0^2 \frac{\nabla^2(\sin^2\theta_0)}{\sin\theta_0},$$
$$\hat{H}_2 = -\hat{\Delta}_m + \left(\frac{l_0^2}{r^2} - 1\right)\cos 2\theta_0 + h\cos\theta_0, \tag{8}$$
$$\hat{V} = \frac{2l_0^2\cos\theta_0}{r^2},$$

where $\hat{\Delta}_m = -l_0^2\nabla^2 + m^2 l_0^2/r^2$, ∇^2 is the radial part of the Laplace operator. Note the "potentials" in these Schröedinger-like operators are not small but localized near the vortex core. The nonlocal magnetostatic effects are included in the integral operators,

$$\hat{U}_1 = -\frac{1}{4\pi M_s}\frac{\partial\Phi}{\partial r} \quad \text{and} \quad \hat{U}_2 = \frac{m\cos\theta_0}{4\pi M_s r}\Phi. \tag{9}$$

To proceed in the solution of Eqs. (7), the asymptotics (4) for the cone-state vortex are used to obtain the expression for f far from the vortex core

$$f = \frac{g}{1 - h^2}\left(\Omega - \frac{2mhl_0^2}{r^2}\right) - \frac{mh}{4\pi r M_s}\Phi. \tag{10}$$

Note here two terms proportional to the external field, which are of crucial importance for the cone-state vortex dynamics. Using (10), the equation for g can be presented as

$$\frac{\Omega^2}{1 - h^2}g = \hat{H}_1^{(\nu)}g - \frac{1}{4\pi M_s}\frac{\partial\Phi}{\partial r} + \frac{mh\Phi}{4\pi r M_s(1 - h^2)}\left(\Omega - \frac{2mhl_0^2}{r^2}\right), \tag{11}$$

where the operator $\hat{H}_1^{(\nu)}$ has the same form as $\hat{H}_1$ in Eq. (8), but with noninteger index $\nu^2 = m^2 + 4mh\Omega/(1 - h^2)$ in the differential operator $\hat{\Delta}_m$. Furthermore, note the value of ν depends on the sign of m that will produce additional splitting of doublets with $m = \pm|m|$, see below. The eigenfunctions, $g_0 = J_\nu(kr) + \sigma_\nu Y_\nu(kr)$, ($J_\nu$ and Y_ν are Bessel and Neumann functions of noninteger index) are known [7] for the case when $\Phi = 0$, $\hat{H}_1^{(\nu)}g_0 = (kl_0)^2 g_0$. To obtain eigenfrequencies for nonzero Φ for any value of m and h, we will use small parameters such as the aspect ratio, L/R, as well as vortex core radius, l_0/R.

To derive the boundary conditions, the edge contribution to the energy can be evaluated by integration of Eq. (2) using the above ansatz with $-\mu(r, \chi, t)|_{r=R}$ as the edge surface charge density. This gives the edge magnetostatic field $H_r = -RLM_s\sin(m\chi + \omega t)F(r, R)g(R)$, where the function F is defined by the angular integral

$$F(r, R) = \int_0^{2\pi} \frac{(R\cos\alpha - r)\cos m\alpha}{(R^2 + r^2 - 2Rr\cos\alpha)\sqrt{R^2 + r^2 - 2Rr\cos\alpha + L^2/4}}d\alpha. \tag{12}$$

The edge field, being formally proportional to small parameter L, has singular behavior near the dot edge, $F(r, R) \to 2\pi R/L \gg 1$ for $R - r \leq L$, and is rapidly decaying as $R/(R - r)$ for $R - r \gg L$. Thus, the edge magnetostatic field is sharply peaked at the disk edge and it gives the effective boundary condition [8], which can be written as

$$\frac{dg}{dr}|_{r=R} + I_m\frac{L}{4\pi l_0^2}g(R)\int_0^R F(r, R)rdr = 0, \tag{13}$$

where $I_m = 2$ for $m = 0$ and $I_m = 1$ for $m \neq 0$. It is stressed here that this boundary condition includes both the exchange interaction (since it contains the exchange length, l_0, as well as the edge magnetostatic contribution). Thus, two nonsmall contributions, from the region of the vortex core and from the dot edge field, are accounted for exactly.

Now a perturbation theory is used for the nonsingular volume magnetostatic field only. The volume part of the potential can be shown to be $\Phi_v = \int_{R_i}^{R_o} dr' S(r, r')(\nabla \cdot M)/M_s$, where

$$S(r, r') = \int_0^{2\pi} d\alpha \cos m\alpha \ln\left|\frac{\sqrt{r^2 + r'^2 - 2rr'\cos\alpha + L^2/4} + L/2}{\sqrt{r^2 + r'^2 - 2rr'\cos\alpha + L^2/4} - L/2}\right|. \tag{14}$$

Assuming that the quantities, l_0^2/R^2 and L^2/R^2 are small, the potential can be written approximately through $g(r)$,

$$\Phi_v = M_s \int_{R_i}^{R_o} S(r,r') \left\{ [r' g(r')]_{r'} + \frac{hm\Omega}{1-h^2} g(r') \right\} dr'. \quad (15)$$

To calculate the frequency, it is assumed that $g \cong g_0$, and multiplication of Eq. (11) by $rg(r)$ and integration over r results in the quadratic equation $a\Omega^2 + b\Omega + c = 0$ to be solved for Ω, where the coefficients are

$$a = \frac{1}{1-h^2} \langle r g_0^2(r) \rangle - \frac{m^2 h^2}{4\pi(1-h^2)^2} \langle\langle g(r) S(r,r') g(r') \rangle\rangle, \quad (16a)$$

$$b = -\frac{mh}{4\pi(1-h^2)} \left\langle \langle g(r) S(r,r') \frac{d}{dr'} [r' g(r')] + L r g(r) F(r,r') g(r') \rangle \right\rangle, \quad (16b)$$

$$c = -(kl_0)^2 \langle r g_0^2(r) \rangle - \frac{L}{4\pi} \left\langle \langle r g(r) F(r,r') \frac{d}{dr'} [r' g(r')] \rangle \right\rangle, \quad (16c)$$

where $F(r,r')$ is determined by Eq. (12), and to shorten equations we denote

$$\langle f(r) \rangle \equiv \int_{R_i}^{R_o} f(r) dr \quad \text{and}$$

$$\langle\langle f(r,r') \rangle\rangle \equiv \int_{R_i}^{R_o} dr \int_{R_i}^{R_o} f(r,r') dr'.$$

All of these results are general and valid for both dots and rings in an external field. The main differences between these two structures appear in the form of the parameter σ_m and the lower limit of integration, R_i. For the case of the ring, the boundary conditions on two edges (R_o and R_i) result in two equations that give both σ_m and k. For dots having an out-of-plane core, the scattering amplitude $\sigma_m = \sigma_m(k)$ is determined [7] by the core region. It is maximal for $|m| = 1$,

$$\sigma_{|m|=1} = -\pi k l_0(m)(1+h)/4 \quad (17)$$

and small [9,10] for $|m| \neq 1$, $\sigma_{|m|\neq 1} \propto (kl_0)^{2|m|}$, for all other values of m. The effective boundary condition on the dot edge $r = R_o$, together with the known dependence, $\sigma_m(k)$, gives both parameters in the radial eigenfunction, σ_m and k. A plot of the left-hand side of Eq. (13) versus k will show an oscillatory function with the zeros giving the values of the wave number. When $m = -1$ the boundary condition exhibits the first zero at $k \approx l_0/R^2$, and it has been shown earlier [8,11,12] that this gives the low-frequency gyrotropic mode. The second zero corresponds to a higher frequency mode. Since there will be two values of k corresponding to $\pm m$, the higher frequency modes with $m \geq 1$ are doublets.

The key point of this Letter is the doublet splitting of the high frequency modes that can occur for both dots and rings. For the following we will use the parameters for permalloy ($l_0 = 4.8$ nm and $4\pi\gamma M_s = 28.4$ GHz) with $R_o = 200$ nm and $L = 50$ nm, which are typical values [3,4] that have been used by other experimental groups.

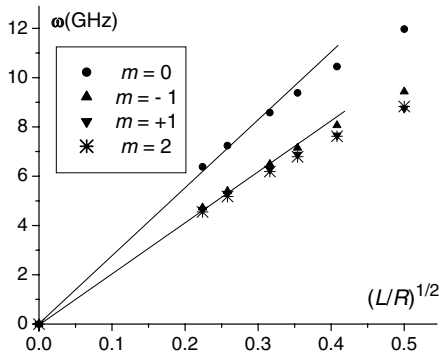

FIG. 1. Frequency of the $m = 0$, $m = \pm 1$, and $|m| = 2$ modes versus $\sqrt{L/R}$ for permalloy dots. Here and in Fig. 2 the straight lines are guides to indicate deviations from linearity.

First consider the zero-field higher frequency modes of the dot calculated from Eqs. (16). The frequencies of modes corresponding to $m = 0$, $m = \pm 1$, and $m = 2$ are obtained by numerical integration of the coefficients given by Eq. (16) and are shown as a function of the aspect ratio in Fig. 1. Notice that the radially symmetric $m = 0$ mode has the highest frequency, and this frequency also agrees [3] with the frequency of the same mode observed using BLS techniques. It is noticed that the frequencies are approximately linear functions of $\sqrt{L/R}$ for small values of the aspect ratio, with larger deviation from linearity as the aspect ratio increases. The doublet splitting is an increasing function of the aspect ratio L/R; it is maximal for $m \pm 1$ modes, and the splitting for $|m| > 1$ modes is not noticeable on this scale because of the small scattering amplitude.

For the case of the dot, Fig. 2 shows the splitting at zero field versus aspect ratio for the $m = \pm 1$ doublet. In addition, the gyrotropic frequency calculated previously [12,13] is also shown on this figure. Note both quantities are the same order of magnitude; moreover, both are approximately linear functions of the aspect ratio. The

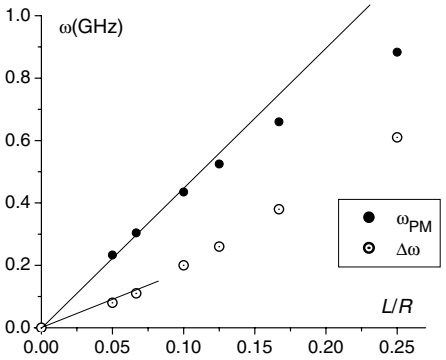

FIG. 2. Frequency of the low-frequency gyrotropic mode ω_{PM} and the magnitude of the $m = \pm 1$ doublet splitting $\Delta\omega$ as a function of L/R for permalloy dots.

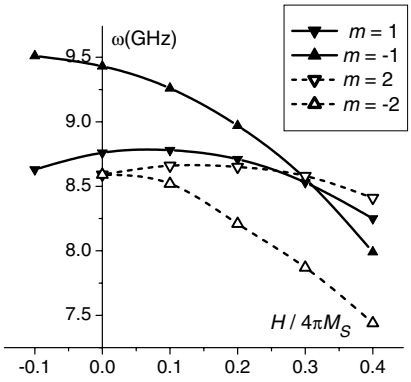

FIG. 3. Frequencies of the $m = \pm 1$ and $m = \pm 2$ modes versus magnetic field for the $R = 200$ nm permalloy magnetic dot of thickness $L = 50$ nm. In Figs. 3 and 4 the triangle symbols are used to distinguish between these curves.

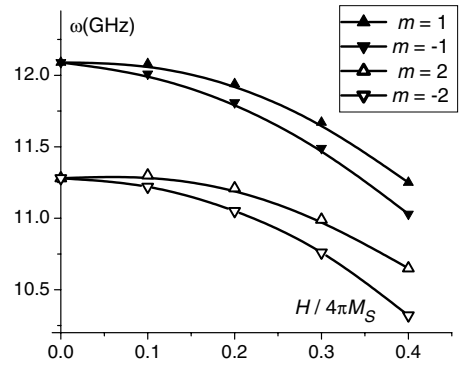

FIG. 4. Frequencies of the $m = \pm 1$ and $m = \pm 2$ modes versus magnetic field for the permalloy magnetic ring with inner and outer radii $R_i = 100$ nm and $R_o = 200$ nm, and thickness $L = 50$ nm.

$m = \pm 1$ modes are the most interesting because of the presence of a significant zero-field splitting, and also this mode has recently [5,6] been observed, but the doublet structure has not yet been reported. For this case the field direction is defined relative to the direction of the core magnetization $\cos\theta_0(0) = \pm 1$ with positive values of h corresponding to parallel alignment and negative values corresponding to antiparallel alignment. The field dependence of the splitting of the $|m| = 1$ and the $|m| = 2$ modes in the dot are illustrated in Fig. 3. Notice that the splitting of the $|m| = 1$ mode will be increased to about 1 GHz when $h \approx -0.1$, which is in the range that can be attained in typical experimental setups. Also notice that the $|m| = 2$ splitting increases with increasing values of h, and the splitting is symmetric in h because of the small value of σ for these higher modes.

For rings, the case of nonzero h is more complicated than the zero-field case. This is because the unknown, Ω, also appears in the boundary condition at the edges, R_i and R_o, as well as in Eqs. (16). To obtain Ω, an iterative procedure is used where the initial choice for Ω is the zero-field frequency with the field increased by a small $\Delta h \approx 0.04$ increment to obtain the next estimate. This is then used in the boundary condition to get new k (and σ), which are used in Eqs. (16) to find the next estimate of Ω. Then this estimate of Ω is used as an initial estimate with h further increased by a small increment. For all values of the field considered here, only two iterations are necessary for the calculated frequency to converge. Finally, the frequencies of the $|m| = 1$ and $|m| = 2$ modes for magnetic ring with $R_i = 100$ nm as a function of h are shown in Fig. 4. Because there is no out-of-plane core, there is no zero-field splitting, and the frequencies are symmetric in h. Notice also that even for rather large values of the field, the magnitudes of the splitting calculated here are rather small and probably not observable by BLS, but its observation is possible by time-resolved Kerr microscopy.

In summary, there is a rich spectrum of magnon modes in vortex-state systems excited by an external pulse, and most of these are doublets. It is expected that these doublets will be detected in the near future by use of a technique such as Kerr microscopy. However, owing to experimental limitations on the frequency resolution, we have shown that the best conditions include large values of L/R in combination with an external field. For applications involving dots or rings in an array, the modes described here can possibly have an effect on the magnetic structure of the array through collective modes in the array. This is the subject of future research.

This research was supported by the National Science Foundation under Grants No. DMR-9972507 and No. DMR-9974273.

[1] R. Skomski, J. Phys. Condens. Matter **15**, R841 (2003).
[2] M. Kläui, C. A. F. Vaz, L. Lopez-Diaz, and J. A. C. Bland, J. Phys. Condens. Matter **15**, R985 (2003).
[3] V. Novosad, M. Grimsditch, K. Yu. Guslienko, P. Vavassori, Y. Otani, and S. D. Bader, Phys. Rev. B **66**, 052407 (2002).
[4] J. P. Park, P. Eames, D. M. Engebretson, J. Berezovsky, and P. A. Crowell, Phys. Rev. B **67**, 020403R (2003).
[5] M. Buess, R. Höllinger, T. Haug, K. Perzlmaier, U. Krey, D. Pescia, M. R. Scheinfein, D. Weiss, and C. H. Back, Phys. Rev. Lett. **93**, 077207 (2004).
[6] S. B. Choe, Y. Acremann, A. Scholl, A. Bauer, A. Doran, J. Stöhr, and H. A. Padmore, Science **304**, 420 (2004).
[7] B. A. Ivanov and G. M. Wysin, Phys. Rev. B **65**, 134434 (2002).
[8] B. A. Ivanov and C. E. Zaspel, Appl. Phys. Lett. **81**, 1261 (2002).
[9] B. A. Ivanov, H. J. Schnitzer, F. G. Mertens, and G. M. Wysin, Phys. Rev. B **58**, 8464 (1998).
[10] D. D. Sheka, I. A. Yastremsky, B. A. Ivanov, G. M. Wysin, and F. G. Mertens, Phys. Rev. B **69**, 054429 (2004).
[11] N. A. Usov and L. G. Kurkina, J. Magn. Magn. Mater. **242-245**, 1005 (2002).
[12] K. Yu. Guslienko, B. A. Ivanov, Y. Otani, H. Shima, V. Novosad, and K. Fukamichi, J. Appl. Phys. **91**, 8037 (2002).
[13] B. A. Ivanov and C. E. Zaspel, J. Appl. Phys. **95**, 7444 (2004).